Phase Gradient Autofocus—A Robust Tool for High Resolution SAR Phase Correction

D. E. WAHL
P. H. EICHEL, Member, IEEE
D. C. GHIGLIA
C. V. JAKOWATZ, JR., Member, IEEE
Sandia National Laboratories

The phase gradient autofocus (PGA) technique for phase error correction of spotlight mode synthetic aperture radar (SAR) imagery is examined carefully in the context of four fundamental signal processing steps that constitute the algorithm. We demonstrate that excellent results over a wide variety of scene content, and phase error function structure are obtained if and only if all of these steps are included in the processing. Finally, we show that the computational demands of the full PGA algorithm do not represent a large fraction of the total image formation problem, when mid to large size images are involved.

Manuscript received June 18, 1992; revised April 9, 1993.

IEEE Log No. T-AES/30/3/16653.

Authors' address: Sandia National Laboratories, P.O. Box 5800, Division 5912, Albuquerque, NM 87185.

I. INTRODUCTION

The ability of a synthetic aperture radar (SAR) to form a high resolution image is dependent on maintaining subwavelength knowledge of platform position from pulse to pulse during the aperture generation time. As imaging standoff distances and aperture generation times increase, the need to measure and accurately track the antenna phase center puts an extreme burden on any motion compensation system. In addition, phase perturbations due to propagation effects can destroy the utility of high resolution imagery, even with perfect motion compensation.

In a typical SAR application, an inertial measurement system is used to sense platform motions over some range of frequencies. These may then be removed from the data prior to image formation [1]. For motion errors beyond the measurement capabilities of inertial measurement units or for propagation induced errors, it is necessary to use data-driven autofocus techniques [2, 3].

It seems unlikely then, that any high resolution SAR system will fully meet its ultimate utility without some means for automatically focusing the imagery, independent of the source or the form of the phase error. Simple automatic focusing methods have been proposed and built since the early days of SAR development. However, these techniques and extensions thereof, that basically track low-order polynomial-like motion errors, have not kept pace with the requirements. High-order phase-error correction has usually been relegated to postprocessing techniques generally requiring human intervention. In addition, it has been difficult to focus scenes containing these errors without having strong isolated scatterers present.

Since the initial publication of phase gradient autofocus (PGA) [4], the algorithm has seen widespread utilization throughout the SAR community. PGA has been demonstrated, by ourselves and others in the SAR community, to provide near diffraction-limited performance on a wide variety of real-world images. SAR designers now have a practical tool by which phase-degraded imagery can be restored to designed impulse response (IPR) specifications in nearly all cases. It is important to note that this performance is achieved with PGA independent of SAR scene content. Specifically, bright isolated point-like reflections are not needed. Therefore scenes completely devoid of cultural features can be restored.

Some concern has been levied toward PGA in terms of its purported computational burden. A natural technical question now arises. Is it possible to shortcut or circumvent any of the processing steps within the PGA construct for the sake of computational efficiency? Several autofocus methods have been proposed that embody a subset of the algorithmic steps of PGA [5–7], but in our opinion, they have

failed to achieve an acceptable level of performance. Our experience with PGA has led us to expect nearly diffraction-limited restoration on virtually any phase-degraded SAR image. Any autofocus algorithm that fails to meet this expectation is simply inadequate.

We intend to show, via processing of real SAR imagery, that nearly diffraction-limited restorations should *always* be expected, even in apparently very difficult autofocus situations. We also show that elimination of any PGA processing step yields unacceptable results in view of our current expectations. Finally, we show that PGA can be implemented to require a fixed amount of data and calculations which becomes a smaller and smaller fraction of the computational load for large image formation problems. In other words, the computational load of PGA does not have to scale with image size as do some other proposed autofocus methods.

We also provide at no cost to other researchers, the entire complex SAR imagery data set used for the examples in this work. We hope that this will foster productive scientific exchange in this fascinating signal processing area and provide a common and realistic set of imagery from which comparative performance can be easily judged.

II. WHY PGA WORKS

Previous publications [4] described the algorithmic steps and phase estimation process of PGA and these are not repeated here in the same detail. We want to take a closer look at the "bigger picture," namely those important constructs and processing steps that make PGA work.

The fundamental concept from which PGA was developed was to make a robust estimation of the derivative (gradient) of the phase error using only the defocused complex SAR image.[1] The estimation process exploits the redundancy of the phase-error information contained in the degraded image, independent of the underlying scene content. In our opinion, there are four crucial processing steps required to allow robust phase-error estimation and image restoration. These four processing steps are referred to as center (circular) shifting, windowing, phase gradient estimation, and iterative correction.

There are several ways to implement the various algorithmic steps. We choose to begin the process with the complex phase-degraded SAR image. This implies that it is not necessary to know how the SAR image was formed, only that the image be phase coherent over the entire scene to be processed. In other words the complex image and phase history are Fourier transform pairs.[2] The range-compressed phase-history domain data are obtained by a one-dimensional Fourier transform in the azimuth (or cross-range) direction.

Let us denote the range-compressed phase-history domain data containing the phase error as

$$F_n(u) = |F_n(u)| \exp\{j[\phi_n(u) + \phi_\epsilon(u)]\}. \quad (1)$$

The subscript n refers to the nth range bin, u is the relative position along the synthetic aperture, $|F_n(u)|$ and $\phi_n(u)$ are the magnitude and phase, respectively, of the range-compressed data for range bin n. The uncompensated error $\phi_\epsilon(u)$ along the synthetic aperture is common to all range bins of interest and independent of n.

After azimuth compression (Fourier transformation), each line of image data consists of a sum [10],

$$F\{F_n(u)\} = \sum_m h(x) * a_{m,n} s(x - x_{m,n}) \quad (2)$$

where $h(x) = F\{\exp[j\phi_\epsilon(u)]\}$ is the transform of the complex aperture phase-error function, the $a_{m,n}s(x - x_{m,n})$ are the scatterer-induced impulse response functions, and * denotes convolution.

A. Circular Shifting

The first step in PGA is to select for each range bin n the strongest scatterer a_n and shift it to the origin (center of the image), to remove the frequency offset due to the Doppler of the scatterer. This shifting operation is done as a circular buffer where samples that would be shifted off the left or right edge of the array, are instead wrapped around and shifted in from the opposite edge. At first glance it appears that the circular shifting operation is doing nothing more than a crude attempt to align the isolated impulse responses of individual scatterers. If SAR images consisted solely of isolated targets, the circular shifting would indeed attempt to align them for each range bin. However, highly defocused images rarely contain isolated scatterers (nonoverlapping point spread functions). In addition, many SAR images consist solely of clutter-like objects, such as trees, grass, dirt roads, rocky and brushy fields, etc. It is important to be able to focus scenes like these as well.

It appears that the circular shifting operation not only attempts to align strong scatterers, subsequently improving the signal-to-noise ratio for phase estimation, but it also aligns regions undergoing subtle contrast changes. Clutter-like scenes consist almost entirely of ill-defined contrast variations whose edge response contains information about the phase-error

[1] Other SAR algorithms have been developed that compute the phase gradient obtained from the Wigner-Ville distribution [8, 9]. These algorithms, however, do not exploit redundancy of phase error information as does PGA.

[2] This condition is always met in spotlight-mode SAR, but modifications to PGA are required to accommodate conventional strip-map imagery.

blurring function. Proper alignment of these low contrast edges is crucial to maximizing the accuracy of the phase-error estimation process. Circular shifting, however, is only one part in the process of robust phase-error estimation and must be complemented by the operations that follow.

B. Windowing

The next important step is windowing the circularly shifted imagery. Windowing has the effect of preserving the width of the dominant blur for each range bin while discarding data that cannot contribute to the phase-error estimation. This allows the phase-error estimation to proceed using input data having the highest signal-to-noise ratio.

The question remains as to how to choose the proper window size W, i.e., how to distinguish between that data associated with the dominant blur and the surrounding clutter. For images containing many strong (non-clutter-like) scatterers such as buildings, vehicles, metallic structures, etc., the signal-to-clutter ratio even for severely blurred scenes is large enough to allow automatic window determination. To do automatic windowing we again exploit the fact that the phase error we seek is redundant in the image. Thus, the brightest scatterer on each range bin is subjected to an identical blurring function. We can therefore estimate the width of his blur W, by registering the dominant blur on each range bin and averaging over the bins. Since the circular shifting operation already performed the registration, we just need to incoherently sum over the range bins to obtain a one-dimensional function whose width at some chosen level adequately captures the support of the point spread function. Mathematically, this one-dimensional function is computed as

$$s(x) = \sum_n |f_n(x)|^2 \tag{3}$$

where $f_n(x)$ is the circularly shifted image data.

Because of the registration, $s(0)$ will be the maximum over x. Furthermore, because of the redundancy of the blur function, $s(x)$ will typically exhibit a plateau approximately W in width and be significantly smaller outside this region. Thus, W can be estimated from $s(x)$ using a variety of methods. We have chosen to measure W by thresholding $s(x)$ at the point 10 dB down from its peak, $s(0)$, then increasing this width by 50%. The window width will decrease for subsequent iterations because the image is becoming more focused. The progress of the automatic window can be monitored as a means for assessing convergence. At convergence, W is typically a few (i.e., 5–6) pixels wide.

When the scene to be focused has low dynamic range and consists almost entirely of clutter-like objects, the automatic window determination method breaks down. This is because the low contrast point and edge response functions do not rise sufficiently above the surrounding clutter to allow proper thresholding of $s(x)$. We have found that a progressively decreasing window width works quite well for low contrast scenes. The initial window width is selected to span the maximum possible blur width (which could be several hundred samples for extremely defocused imagery) and progressively reduced by 20% for each iteration.

C. Phase Gradient Estimation

After the image data is circularly shifted and windowed, the phase gradient is estimated. Let us denote the shifted and windowed image data as $g_n(x)$ and $G_n(u) = |G_n(u)|\exp(j[\phi_\epsilon(u) + \theta_n(u)])$ be the inverse Fourier transform. The scatterer-dependent phase function for each range bin is denoted by $\theta_n(u)$.

It has been shown [10] that a linear unbiased minimum variance (LUMV) estimate of the gradient of the phase error, $\phi_\epsilon(u)$, is given by,

$$\begin{aligned}\hat{\dot{\phi}}_{\text{lumv}}(u) &= \frac{\sum_n \text{Im}\{G_n^*(u)\dot{G}_n(u)\}}{\sum_n |G_n(u)|^2} \\ &= \dot{\phi}_\epsilon(u) + \frac{\sum_n |G_n(u)|^2 \dot{\theta}_n(u)}{\sum_n |G_n(u)|^2}.\end{aligned} \tag{4}$$

Thus, this LUMV estimate yields the gradient of the true phase error, plus an error term that has been made as small as possible (at this step) by the circular shifting and windowing operations.

The PGA phase gradient estimation kernel is defined as the second term in the above equation. This kernel is only one of a number of phase gradient, phase derivative, or phase difference estimation formulas. For example, another kernel used to estimate phase differences is given by

$$\Delta\hat{\phi}_\epsilon = \arg\left\{\sum_n F_n(u + \Delta u)F_n^*(u)\right\}. \tag{5}$$

This kernel is found in the Knox-Thompson method for stellar speckle interferometry and in the shear averaging technique for SAR phase-error correction [5]. It has been shown that this kernel is a maximum likelihood estimate of the phase and does work well when used within the full PGA construct [11]. Without the processing steps of center shifting, windowing and iteration, this kernel as well as the PGA kernel will not uniformly produce excellent results over a variety of scene content and phase-error functions.

D. Iterative Phase Correction

The estimated phase gradient, $\hat{\dot{\phi}}_{\text{lumv}}(u)$ is integrated to obtain $\hat{\phi}_\epsilon(u)$, and any bias and linear trend is removed prior to correction. Phase correction

is imposed by complex multiplication of the range-compressed phase-history domain data by $\exp[-j\hat{\phi}_\epsilon(u)]$. The estimation and correction process is repeated iteratively. As the image becomes more focused, individual scatterers become more compact, the signal-to-clutter improves, the circular shifting more precisely removes the Doppler offsets, and the algorithm is driven toward convergence. Removal of any linear trend in the phase-error estimate prevents image shifting and the bias removal allows computation of the rms phase error removed at each iteration as a means for monitoring convergence. Our experience has shown that when the rms error drops to a few tenths of a radian, the image is well focused and will not improve with additional iterations.

III. PROOF OF NECESSITY

The critical steps of the PGA algorithm consist of center shifting, windowing and phase gradient estimation. These steps are repeated iteratively until the algorithm converges to the true phase error. This section illustrates the necessity of all these steps by showing the effect of the PGA focusing algorithm when any of these critical steps are eliminated. By doing this experiment, we show by counter example that the quality of the resultant image is inferior to that which can be achieved by using the full PGA process.

We approach the problem by focusing an image with only one of the critical steps eliminated from the PGA algorithm. The focused result can then be compared with the result using the full PGA algorithm. There are three possibilities using this approach: PGA without center shifting, PGA without windowing, and PGA without iterating. (Although phase gradient estimation is stated as one of the steps of PGA, it is the heart of this phase correction process and thus cannot be eliminated as one of the possibilities in our experiment.)

A typical SAR image was selected for the example. The image is that of a rural scene with no apparent cultural targets. The image was artificially corrupted by a tenth-order phase error.

The following four examples illustrate the effect of implementing a subset of the PGA algorithm on this phase corrupted image. Case 1 implements the PGA algorithm without iterating. In other words, one pass was done which included center shifting and windowing at 1/3 the aperture size before the PGA kernel was used to estimate the phase errors. Case 2 deletes the windowing step from the PGA algorithm. This case was implemented by leaving the window wide open. At each iteration, the brightest point on each range bin was circularly shifted to the center of the image before using the PGA kernel to estimate the phase error. In case 3, the circularly shifting process is removed. The windowing was implemented by reducing the window size by 1/3 at each iteration. Finally, Case 4 implements the full PGA algorithm.

TABLE I
Case Parameters, rms Errors and Associated Fig. Number

Case Number	C.S.	Wind	Iteration	rms (rads)	Fig.
1	Y	Y	N	3.92	1(c)
2	Y	N	Y	1.69	1(d)
3	N	Y	Y	11.2	1(e)
4	Y	Y	Y	0.53	1(f)

The original and the phase-corrupted images are shown in Figs. 1(a) and (b), respectively. The focused result of the algorithms described in cases 1–4 are shown in Figs. 1(c)–(f). By visually comparing the focused results, it is clear that the best result is produced by the algorithm using all the PGA steps. Additionally, an rms value of the original phase error subtracted from the estimated phase error for each case was calculated. The rms value of the applied phase error is 5.61 rads. These results are shown in Table I.

The rms errors and the visual comparisons of the focused results indicate that eliminating any of the steps of the PGA algorithm produces an inferior quality focus. These experiments show that for at least one SAR image, any algorithm claiming computational advantage over PGA by essentially eliminating one or more steps of PGA produces results which are suboptimal. Although these results are specific to one image, it has been the authors experience that all the steps are required in order to achieve high quality focus on the vast majority of SAR images.

IV. ROBUSTNESS OF PGA

It is of course impossible to predict and test every conceivable phase-error function and scene content combination to demonstrate the infallibility of any autofocus algorithm. The authors, however, feel the PGA algorithm is exceedingly robust over a wide range of applications. This confidence is born of analysis using optimal estimation theory [10], as well as its application to a large number of fielded SAR systems by the authors and others. In this section, we present the results of applying PGA to a variety of scenes and phase-error functions to demonstrate this robustness. As in the previous section, all of these examples were generated using actual SAR imagery with synthetic phase-error functions applied.

It has been asserted that PGA is a discrete point-type algorithm generalized to average over many such points. Indeed, the analysis cited above models a SAR image as a collection of such points for the sake of mathematical tractability. However, the PGA algorithm has demonstrated its ability to focus an image in the complete absence of dominant reflectors

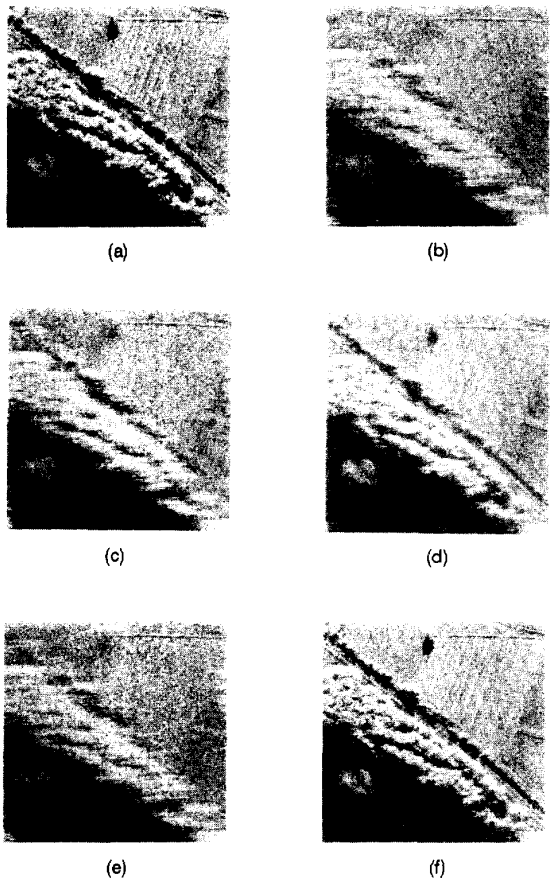

Fig. 1. SAR image of field and trees. (a) Original, undegraded. (b) Corrupted with 10th-order polynomial phase error. (c) Case 1, no iteration. (d) Case 2, no windowing. (e) Case 3, no circular shifting. (f) Case 4, full PGA algorithm.

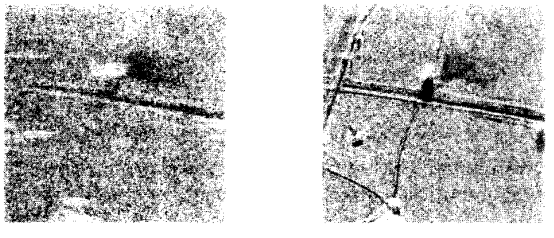

Fig. 2. SAR image of rural scene with no cultural, metallic, or specular targets. (a) Corrupted with 10th-order polynomial phase error. (b) Corrected using PGA.

with sidelobes above the surrounding clutter. Fig. 2 is such an example. The underlying image is one of a rural scene with *no cultural, metallic, or specular targets whatsoever*. Were it not for some tree shadows, this scene would be almost featureless. As can be seen from Figs. 2(a) and (b), PGA has no difficulty removing the substantial phase-error function from this data.

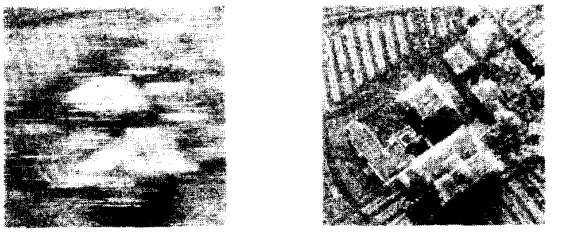

Fig. 3. SAR image of urban scene with dense set of large cross section targets. (a) Corrupted with 10th-order polynomial phase error. (b) Corrected using PGA.

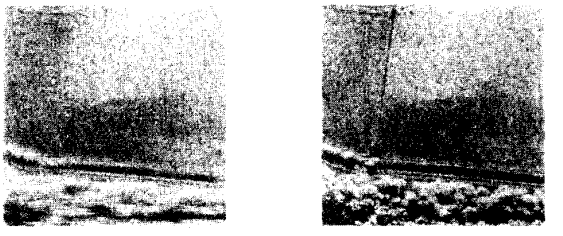

Fig. 4. SAR image of low dynamic range scene. (a) Corrupted by large magnitude phase error function with power law second-order statistics. (b) Corrected using PGA.

Conversely, dense collections of scatterers with intermingled sidelobe structure can be handled as well. That is, if large magnitude scatterers are present, they need not be *isolated*. In Figs. 3(a) and (b), we show the results of applying PGA to an urban scene with a dense set of large cross section targets.

The above three examples possessed tenth-order polynomial phase-error functions (see Fig. 6). This type of phase error might be expected as a residual after the data has been motion compensated (although typically not this severe). Propagation induced phase errors such as that generated by a turbulent ionosphere or troposphere, however, can have much higher frequency components [11]. In this case, it is imperative to use a nonparametric phase-error estimation technique such as PGA. Due to the exponential modulation, large magnitude high frequency phase errors cause severe spreading of the impulse response.

The next example is particularly difficult from the standpoint of phase correction. A low dynamic range scene has been corrupted by a large magnitude phase-error function with power law second-order statistics (see Fig. 7). Thus, use can be made of neither a dominant scatterer nor smoothing by fitting a low-order polynomial to the error function. The efficacy of PGA, however, can be seen in Figs. 4(a) and (b).

The last example is of largely academic interest. Practical SAR systems are designed with adequate

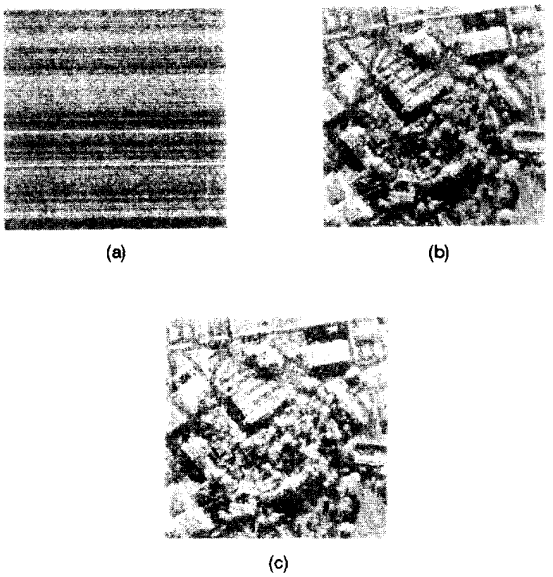

Fig. 5. SAR image on urban scene. (a) Corrupted by white phase error function. (b) Corrected using PGA. (c) Original undegraded image.

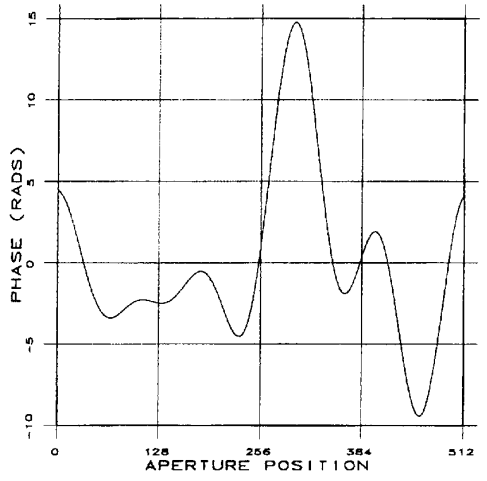

Fig. 6. Tenth-order polynomial phase error function used to produce corrupted images shown in Figs. 1(b), 2(a), and 3(a).

motion compensation/phase stabilization so the phase errors at adjacent azimuth samples will not exceed pi radians. However, a question arises as to what would happen if a *white* phase error function were applied to an image. This function would clearly exceed pi radians at many adjacent azimuth samples producing a spread of the IPR across all azimuth samples. That is, neglecting range walk (which cannot be corrected by autofocus), what are the consequences of a random, white error function? It has been suggested that PGA, with its differential-based estimation kernel, could not handle such a situation. This is not true. In this case,

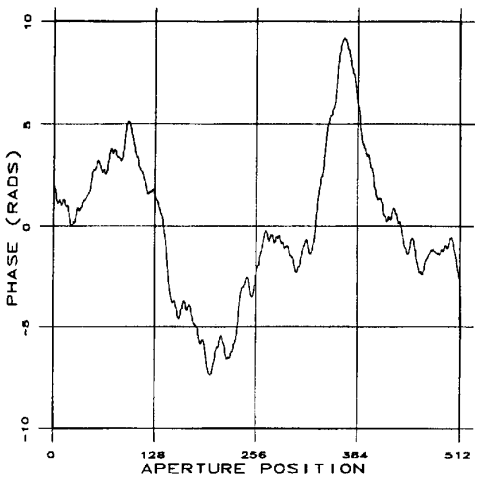

Fig. 7. Power law phase error function used to produce corrupted image shown in Fig. 4(a).

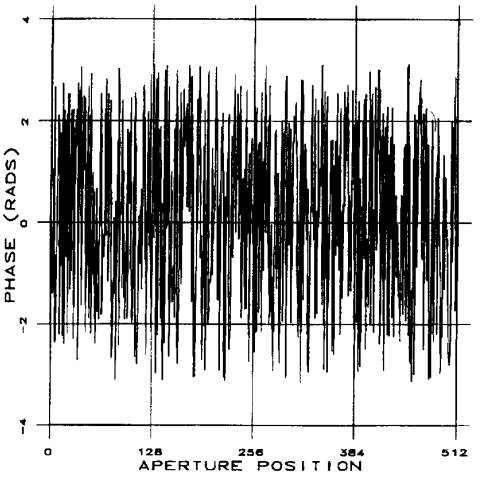

Fig. 8. White phase error function used to produce corrupted image shown in Fig. 5(a).

the estimated phase-error function turns out to be a function with the *same principal values of phase as the original error function* and slopes less than pi radians per sample. Thus, while it is not the same function as that impressed on the image, after the phase wrapping due to $e^{j\varphi}$, it has the same effect on the image. To put it another way, given any aliased, random phase function, it is possible to find an unaliased phase function with the same principal values. The PGA algorithm converges to this function. Fig. 5(a) depicts an urban scene that has been corrupted by a white phase-error function (see Fig. 8). As expected, the IPR has been blurred the entire width of the image. The PGA restored image is shown in Fig. 5(b). This image appears to be about as well focused as the original (Fig. 5(c)).

V. COMPUTATIONAL CONSIDERATIONS

Upon initial inspection, the PGA algorithm appears to be burdensome from a computational standpoint. It is iterative, requires Fourier transforms between the image and range-compressed domains for each iteration, and such processing must be performed over many range bins to take advantage of the redundancy in the data that is the key to the success of the algorithm.

However, in this section we show that a variety of processing expediencies may be employed to dramatically improve throughput. In fact, it is shown that *the processing burden is essentially fixed, independent of image size*, and as such represents a proportionately ever decreasing computational load as image size grows. Thus, in the authors' experience, PGA represents a tiny fraction of image formation time for large images.

In what follows, we consider only the *phase-error estimation* portion of the problem. The final *correction* of the data is generic to the autofocus problem in SAR, and as such, is a fixed computational burden independent of PGA. Further, we consider here only the case of large problem sets. For small SAR images, the economies to be described here would have little impact. In order to fix these ideas, let us exaggerate the point and consider by way of example a very large SAR image of 10 K $\times$ 10 K samples.

There are three fundamental steps that may be taken to reduce the computational burden of PGA. They are: 1) limiting the estimation to a reduced number of range bins, 2) limiting the estimation to a reduced number of cross-range bins, and 3) utilizing variable-length fast Fourier transforms (FFTs).

Consider our hypothetical 10 K $\times$ 10 K sample image, and suppose for the moment that the data have been fully compressed to the image domain. It is unlikely that all 10 K range bins are required to make an excellent estimate of the phase-error function. In fact, our experience has demonstrated that estimation over 500 well chosen range bins is adequate in virtually every circumstance. Likewise, even the most severely degraded or poorly motion-compensated image is likely to suffer less than 500 samples of cross-range impulse response smearing. While this is certainly subject to various system design parameters, the vast majority of SAR systems will nevertheless have an upper bound on IPR smear size.

Consider, then, constructing an image consisting of 500 range samples by 500 cross-range samples taken from the original 10 K $\times$ 10 K image as follows. Locate the 500 highest magnitude samples in the original image. Place these 500 samples in the central column of the 500 $\times$ 500 image. Finally, fill in the samples to the left and right of this central column with the corresponding adjacent samples from the original image, circularly buffering as required. This 500 $\times$ 500 sample "image" so constructed becomes the input image to the PGA algorithm, amounting to a 400 : 1 data reduction at the front end.

This construction may also be accomplished from the range-compressed domain (prior to cross-range compression) in several ways. A set of range bins can be selected based on a rank ordering of total energy in each bin, or by compression of a fraction of the range-compressed data to obtain a low cross-range resolution image. The appropriate cross-range samples may then be obtained by compression of only those selected range bins.

The third computation-saving technique is embedded in the PGA algorithm itself. Since, at every iteration, many cross-range samples are discarded by the windowing operation, it makes sense to perform FFTs on vectors of length equal to the number of non-zero samples retained by the window. This has a dramatic effect on the later iterations as the window sizes become quite small. Of course, the estimated phase-error vector must be up-sampled to the full cross-range dimension to be applied to the range compressed data at each iteration. Also, the final correction vector obtained from this 500 $\times$ 500 sample image must again be up-sampled to the original image size.

If we accept the hypothesis that an input image to PGA has an upper bound of say 500 range samples by 500 cross-range samples (exact numbers depending on system design), then it is clear that the computational burden of PGA does not grow with actual image size above these numbers. On the other hand, virtually every other processing step in SAR image formation (motion compensation, polar formatting, range and cross-range compression, and geometric correction) does grow linearly (or faster) with image size. It is thus easily seen that, while PGA represents a substantial fraction of image formation for small images, it becomes inconsequential for large images.

VI. SUMMARY

The PGA algorithm for phase-error correction in SAR was introduced in 1988. Since that time, it has been proven to be a robust technique that can provide excellent results over a wide variety of both scene content and structure of the degrading phase-error function. Indeed, PGA is capable of restoring defocused SAR images to their designed quality specifications in nearly all instances. The success of the technique relies upon four fundamental signal processing steps. These include center shifting, windowing, phase gradient estimation, and iterative correction. The question has been raised, however, as to whether or not these four elements are in fact crucial to the robustness of the algorithm. Several techniques now exist that utilize a subset of the PGA algorithmic steps. We demonstrate here that

omission of *any* of these basic elements from the PGA construct has deleterious effects on the final product. As a result, we suggest that no shortcuts to PGA are appropriate, since use of the complete PGA technique will essentially always deliver nearly diffraction-limited imagery. We then show that the computational load of PGA is really not a very large fraction of the complete image formation process when mid to large size images are involved. Finally, the digital SAR data sets used here to demonstrate our assertions are offered to other researchers at no cost,[3] in order to stimulate further research in this area. The use of a common set of realistic SAR images should facilitate useful comparative performance studies.

REFERENCES

[1] Kirk, J. C. (1975)
Motion compensation for SAR.
IEEE Transactions on Aerospace and Electronic Systems, (May 1975).

[2] Brown, W. D., and Ghiglia, D. C. (1988)
Some methods for reducing propagation-induced phase errors in coherent imaging systems, Part I, Formalism.
Journal of the Optical Society of America, **5** (June 1988).

[3] Ghiglia, D. C., and Brown, W. D. (1988)
Some methods for reducing propagation-induced phase errors in coherent imaging systems, Part II, Numerical results.
Journal of the Optical Society of America, **5** (June 1988).

[4] Eichel, P., Ghiglia, D., Jakowatz, C., Jr. (1989)
Speckle processing method for synthetic-aperture-radar phase correction.
Optics Letters, **14** 20 (Oct. 1989).

[5] Fienup, J. (1989)
Phase error correction by shear averaging.
Technical Digest Series, **15**, Signal recovery and synthesis II (June 1989), 134–137.

[6] Attia, E. H., and Steinberg, B. D. (1989)
IEEE Transactions on Antenna Propagation, **37** (1989), 30–38.

[7] Press, W. (1991)
Recovery of SAR images with one dimension of unknown phases.
JASON report JSR-91-175.

[8] Barbarossa, S., and Farina, A. (1992)
Detection and imaging of moving objects with SAR, Part 2; Joint time-frequency analysis by Wigner-Ville distribution (WVD).
IEE Proceedings, Pt. F, **139**, 1 (Feb. 1992).

[9] Barbarossa, S. (1990)
New autofocusing technique for SAR images based on the Wigner-Ville distribution.
Electronics Letters, **26**, 18 (Aug. 1990).

[10] Eichel, P., and Jakowatz, C., Jr. (1989)
Phase-gradient algorithm as an optimal estimator of the phase derivative.
Optics Letters, **14**, 20 (Oct. 1989).

[11] Jakowatz, C., Jr., and Wahl, D. E. (1993)
Eigenvector method for maximum-likelihood estimation of phase errors in synthetic-aperture-radar imagery.
Journal of the Optical Society of America, **10** (Dec. 1993).

[12] Jakowatz, C., Jr., Eichel, P., and Ghiglia, D. (1989)
Autofocus of SAR imagery degraded by ionospheric-induced phase errors.
SPIE, **1101** (1989).

[3]Send postage prepaid mailing envelope with a QIC (1/4" cartridge) tape to the authors at the above address.

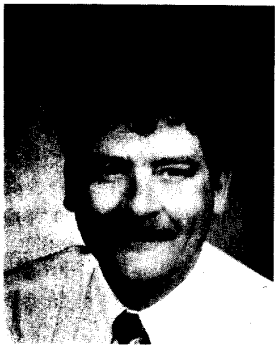

Daniel E. Wahl received his B.S. and M.S. degrees in electrical engineering from Colorado State University, Ft. Collins, in 1981 and 1983, respectively and the Ph.D. degree from the University of New Mexico in electrical/computer engineering in 1993.

Since 1983 he has been a senior member of the technical staff at Sandia National Laboratories, Albuquerque, NM. His current interests include digital signal and image processing, synthetic-aperture radar signal processing, and SONAR array signal processing.

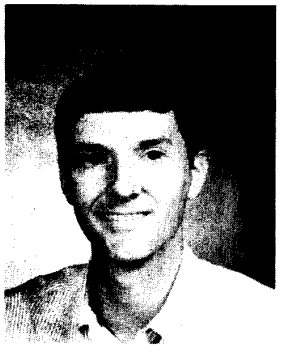

Paul H. Eichel (S'77—A'79—M'85) received the B.E. degree from Vanderbilt University, Nashville, TN in 1978, the M.S. degree from Stanford University, Palo Alto, CA in 1979, and the Ph.D. degree from the University of Michigan, Ann Arbor, in 1985, all in electrical engineering.

From June 1978 through August 1981 he was a member of the technical staff at Bell Laboratories, Holmdel, NJ. Since July 1985, Dr. Eichel has been with the Sandia National Laboratories in Albuquerque, NM where he is a distinguished member of the technical staff. His activities and interests include theoretical and experimental aspects of modulation and channel coding, digital signal processing, and synthetic aperture radar.

Dr. Eichel is a member of Tau Beta Pi, the IEEE Information Theory Group, and the IEEE Acoustics, Speech, and Signal Processing Society.

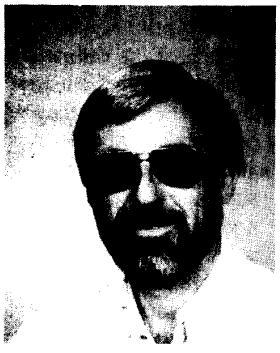

Dennis C. Ghiglia received the bachelor's degree in electrical engineering at California State Polytechnic University, Pomona, in 1969 and the M.S. and Ph.D. degrees in electrical engineering from Arizona State University, Tempe, in 1972 and 1976, respectively.

He is a distinguished member of the technical staff at Sandia National Laboratories, Albuquerque, NM, where he has been employed since June, 1978. He has been responsible for the development of the Image Processing Facility for the centralized support of a wide range of image processing activities. Before joining Sandia, he was employed by Goodyear Aerospace near Phoenix, AZ, where he did signal processing, image processing, and systems analysis for synthetic-aperture radars. His current research interests lie in the area of image restoration, synthetic-aperture radar signal processing, and phase problems in signal and image processing.

Dr. Ghiglia is a member of the Optical Society of America.

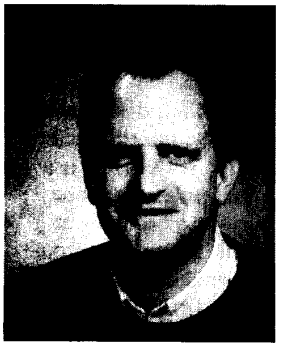

Charles V. Jakowatz, Jr. (S'75—M'90) was born in 1951 and received the B.S., M.S., and Ph.D. degrees, all from the School of Electrical Engineering at Purdue University, W. Lafayette, IN, in 1972, 1973, and 1976, respectively.

He is currently Manager of the Signal Processing Research Department at the Sandia National Laboratories in Albuquerque, NM, where he has been employed since 1976. During his tenure at the national laboratory, his chief research interests have been in digital signal processing, computed imaging, as well as detection and estimation theory. During the past six years, he has worked in R&D for synthetic aperture radars.